

A Study of Photoreactivity of Inorganic Nanocrystals with Significant Organic Colors

K. Umamakeshvari^{1,*}, S.C. Vella Durai², M. Nagarajan³

¹ Christopher Arts and Science College (Women), Nanguneri, Tirunelveli 627108, Tamilnadu, India

² Manonmaniam Sundaranar University College, Govindaperi, Cherenmahadevi, Tirunelveli, 627414
Tamilnadu, India

³ Government Arts and Science College, Kanyakumari, 629401 Tamilnadu, India

(Received 03 September 2022; revised manuscript received 20 October 2022; published online 28 October 2022)

When it comes to photonic optoelectronic materials, colloidal nanocrystals of semiconductor quantum dots (QDs) are quickly rising to the top of the heap. With their great efficiency and narrow emission band, they have gained interest for their usage in artificial lighting and displays because of their spectral purity and fine-tunability. As a result of using QDs in color-conversion LEDs in combination with phosphors, it is possible to simultaneously achieve successful color rendition of illuminated objects. The device spectral overlap with the sensitivity of the human eye is outstanding, in contrast to other conventional sources like incandescent and fluorescent lights and phosphor-based LEDs, which cannot attain all of the above features at the same time. Color science of QDs for lighting and displays is summarized in this paper, along with recent breakthroughs in QD-integrated LEDs and display research. Color science, photometry, and radiometry are introduced in the first chapter. Spectral designs of QD-integrated white LEDs have resulted in efficient lighting for both indoor and outdoor applications after offering an overview of QDs. QD color-conversion LEDs and displays are discussed as proof-of-concept applications in the next section. Finally, we present an overview of research opportunities and difficulties, as well as a prediction for the future.

Keywords: Color science, Displays, Light emitting diodes, Nanocrystals, Photometry, Quantum dots.

DOI: [10.21272/jnep.14\(5\).05023](https://doi.org/10.21272/jnep.14(5).05023)

PACS numbers: 61.46.Hk, 73.21.La, 85.60.Jb

1. INTRODUCTION

Since artificial lighting accounts for almost 20 % of global electricity usage [1] and this number can rise to 30 % in some places, lighting offers great opportunities for energy savings [2]. Solid-state lighting (SSL) holds significant promise for reducing this figure, as it is expected to reduce electricity consumption by 50 % [3]. The US department of energy estimates that switching to light-emitting diodes (LEDs) from all existing light sources will save 133 TWh of electricity annually in the United States [4]. White light, which is created by sources such as incandescent, fluorescent, high-pressure sodium lamps, mercury vapor lamps, and LEDs is required for most general lighting applications. LEDs have received a lot of attention in recent years thanks to their ability to save energy. There are a variety of methods for creating a white light spectrum with LEDs. One option is to employ numerous LED chips that emit distinct colors at the same time; however, this technology has significant limitations that have hindered broad adoption. To begin, there is currently no efficient material system for green LEDs [5]. The final LED lamp price goes up because several chips necessitate complex electrical circuitry. As a result, this strategy falls short in terms of achieving the necessary efficiency and cost effectiveness. As an alternative, color-converting materials can be included on a blue- or near UV-emitting LED chip to produce white LEDs. Today, rare-earth-ion-based phosphors are used to color-convert the majority of white LEDs [6]. Because of this, they have high absorption at short wavelengths and a broad emission range that includes the entire visible spectrum. Energy-efficiency

improvements have made significant headway in recent years. In terms of energy efficiency, other common business lighting options like fluorescent and incandescent bulbs have already been surpassed. Aside from the color quality and spectrum efficiency of the existing white LED phosphors, there are several other issues with contemporary white LEDs. Although individual high performances are feasible, these LEDs cannot provide outstanding color rendition, good spectral match with human spectral sensitivity, and a warm white shade all at the same time [7]. Because of the difficulty in tuning phosphors' wavelengths, this is the primary cause. Phosphor supply and commercial monopoly issues have led to an increase in demand for alternative color converters. It is at this moment that QDs are emerging as a promising candidate because of their ability to precisely adjust their size and narrow-band emission [8]. In other words, by using QDs in white LEDs, it is possible to improve the efficiency of the light source, as well as display objects in their true hues, as well as create a warm white shade and a good spectral overlap with the human eye sensitivity function. They can also contribute to the device high electrical efficiency by virtue of their high photoluminescence quantum efficiencies [9, 10]. QDs offer considerable promise for white LEDs because of their superior color purity, photometric and electrical efficiency. QD-based LEDs can also be utilized as backlights for liquid crystal displays, making them ideal for a variety of applications (LCD). High-purity colors can be reproduced because QDs have a very narrow emission band. The color gamut of the LCDs can also be widened with these materials; in other words, a wider range of colors is possible [9].

* chitra.uma86@gmail.com

1.1 Color-Converting Nanocrystal Quantum Dots

Our daily lives have been transformed by semiconductor-based optoelectronic gadgets, which have become increasingly commonplace in recent years. The development of new structures exploiting quantum mechanical processes has begun as new studies focus on manipulating materials at the nanoscale. One of these structures is colloidal semiconductor nanocrystal QDs [11]. Semiconductor QDs play a vital role in photonics because their effective band gap may be controlled within or close to the visible spectral range simply utilizing one material system. By manipulating their size and distribution, these materials can again modify their optical properties [12]. This means that the development of novel lasers, LEDs, solar cells, and other optoelectronic devices is possible. Since QDs have a small emission range and their highest peak emission wavelength is located within the visible spectral range, these materials hold considerable promise for improving the photometric and colorimetric features of white LEDs [13]. This allows for numerous QD emitters finely tuned one at a time to generate the desired spectrum collectively. As long as the excitation wavelength falls below the band edge of the QD broadband absorption, conventional phosphors with narrow absorption bands have to deal with this issue. Here, we will focus mostly on LED applications, while discussing these materials' physical and chemical features [14].

Increasingly, classical mechanics is no longer sufficient to describe the properties of materials; instead, the governing mechanisms are based on the principles of quantum physics. The same basic principles apply to semiconductor nanocrystal QDs. Electrons and holes in a semiconductor QD are typically restricted to a region of 2-10 nm in three dimensions. In semiconductors,

electrons and holes are typically separated by this distance. Consequently, the crystalline semiconductor electrons and holes begin to see the surrounding free space or any other material with a greater band gap as a barrier. Because the system is limited to a finite quantum well problem, the material properties are determined by the discrete energy levels. Fig. 1 shows a schematic diagram of a QD and its accompanying energy band diagram.

Nanometer-sized semiconductor crystals are shown to have quantum confinement effects via the QDs' emission and absorption spectra. First, the emission spectrum of the semiconductor material shifts significantly bluer than that of the bulk material. There are several differences between a bulk CdSe crystal and its QDs, for example. It is also noteworthy to mention that the QDs' blue shift is highly influenced by the material size. The emission peak shifts toward higher energies and shorter wavelengths when the well width narrows with decreasing QD size. QD size distribution and trap density substantially influence the emission spectrum bandwidth, which is dependent on the QD emission spectrum bandwidth. Absorption features, like emission, show a size-dependent tendency. The absorption begins at greater photon energies or shorter wavelengths as the QD size diminishes. As seen from Fig. 2, QDs have typical emission and absorption spectra.

1.2 Semiconductor Nanocrystal QDs for Light Source Spectral Design

Optimizing white light spectrum is a complex task that must be done in accordance with the application, as discussed in the section on color science and photometry. When designing an indoor light source, for example, the color rendering, spectrum overlap with

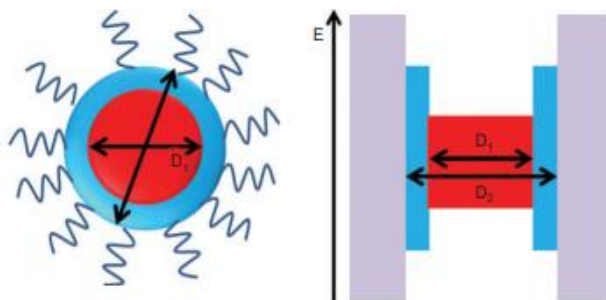


Fig. 1 – Semiconductor QD: core/shell semiconductor QD schematic (left) and band diagram (right)

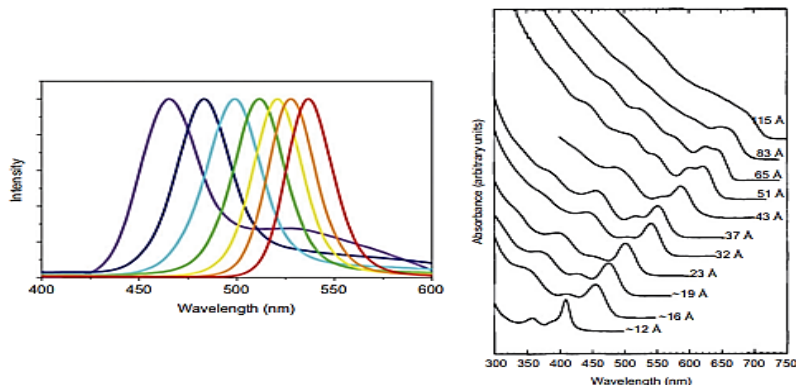


Fig. 2 – Size-dependent characteristics in both the emission (left) and absorption (right) spectra of CdSe QDs

the human eye sensitivity function and warm white shade are all necessary. For outdoor lighting, however, the performance criteria are rather different [15]. Because of the variations in eye sensitivity in the mesopic lighting levels, for example, the luminance has to be raised. High CRI Road illumination may also help drivers see better while behind the wheel. Light sources that affect human circadian cycles, however, necessitate a whole different design [16]. It is important to select the emitters carefully for each application because each application has its own figure of merit, and some applications have complex trade-offs between performance factors. When it comes to generating high-quality light sources, narrow emitters like QDs are ideal, as they give significant freedom in the spectrum design. Spectral design for indoor and outdoor applications using nanocrystal QDs as color-converter materials is brought together in this section of the review spectral characteristics and the trade-offs between relevant figures of merit are examined for indoor lighting applications. Furthermore, a discussion of the potential power conversion efficiency of QD-integrated white LEDs follows. For outdoor lighting design, we have compiled our recent findings on achieving high mesopic luminosity [17]. Finally, we mention white LED spectra with enhanced S/P ratios integrated with QDs.

1.2.1. Spectral Design for Indoor Lighting Using Nanocrystal QDs

Color components must be carefully chosen in order to produce warm white light sources with high CRI and high LER. Having an understanding of the trade-offs between these figures of merit, it is also useful when designing the light source [18]. A Gaussian spectrum model of the emission of nanocrystal QDs was previously used in computational simulations [7]. The white light spectrum was created by combining four color components, namely blue, green, yellow, and red, into a single spectrum. In all, 237,109,375 QD-integrated white LED (QD-WLED) spectra were examined in terms of photometric performance by varying the peak emission wavelength (WL), the full width at half maximum (FWHM), and the relative amplitude of each QD color component. A two-step threshold was set before the findings were examined. Spectra with a CRI > 80, an LER > 350 lm/W opt, and a CCT < 4000 K were chosen first. A comparison of CRI, CCT, and LER performance metrics was made using these results. The LER limit was raised to 380 lm/W opt and the CRI limit was raised to 90. Fig. 3 summarizes the trade-offs between CRI, LER, and CCT, showing that when LER rises, so does the maximum achievable CRI. When operating at a lower CCT, this trade-off becomes more pronounced. It is also necessary to use warmer whites to get maximum CRI for any given LER. Even at higher LER values, the maximum achievable CRIs can only be achieved at cooler white colors.

Besides the tradeoffs, Ref. [7] describes the spectrum requirements for maintaining the warm white emission utilizing QDs in order to achieve high CRI and LER values. To get the best photometric performance, the red color component FWHM must be less than 30 nm wide. In addition, the spectrum should

have a strong red component (about 430/1000) and a faint blue component (around 90/1000). Furthermore, the red color component peak emission wavelength, which needs to be near 620 nm, is determined to be an important characteristic. For achieving great performance, this suggested value is quite important. Nonetheless, the models show that the peak emission wavelengths of blue, green and yellow are around 465, 528 and 570 nm, respectively.

However, the higher standard deviations found allow greater flexibility in choosing these peak emission wavelengths without sacrificing photometric performance. A standard deviation of eight millimeters (nm) can be seen in these color components, giving the designer more freedom in picking these parameters. There is a 229/1000 and 241/1000 average amplitude for each of the green and yellow components with standard deviations of more than 70/1000. For the photometric performance of QD-WLEDs, it is obvious that the selection of the green and yellow relative amplitudes is less important than the standard deviation of blue and red (20/1000 and 49/1000, respectively). For CCT 4000 K and CRI > 90, the spectrum created using the average values stated above for the simulated criteria is 91.3 (CRI), 386 lm/W opt (LER), and 3041 K (CCT) in the spectrum (Fig. 4). In this study, it was found that QD-WLEDs can have very high CRI and LER values while preserving a warm white color.

No consideration was given to the compatibility of the simulations to the ANSI standards or to the rendering of R9 (the special CRI number 9), which may have very low values for LED lighting applications, even though the study in Ref. [19] stated that obtaining a photometrically efficient QD-WLED with good color rendition was possible. A multi-objective evolutionary approach was utilized by Zhong et al. [20] to address these issues, where the R9 value of 90 was used as an extra threshold in addition to the performance limits of CRI \geq 80, LER \geq 300 lm/W opt, and 1500 K \leq CCT \leq 6500 K. Table 1 lists the optimum spectral parameters for determining whether CRI = 95 and R9 = 95, resulting in the maximum LER, and the associated spectra in Fig. 5 show the relevant spectra.

1.2.2. Spectral Designs for Outdoor Lighting Using Nanocrystal QDs

Light sources must be designed with an individual purpose in mind. The tint of white light is not as important in outdoor lighting as it is in inside lighting. A more significant change occurs in the eye sensitivity when driving in low-luminance conditions, where the vision regime shifts to mesopic [21]. This means that any computation of perceived brightness based on the photopic eye sensitivity function cannot provide accurate information about the actual brightness. Instead, the variations in the eye sensitivity function should be taken into consideration when calculating mesopic brightness.

1.3 Semiconductor Nanocrystal QD-WLEDs

This review has largely focused on research into QD-WLED development and its promise for photometry and color quality up until now. We now begin re-

viewing the experimental demonstrations of QD-WLEDs at this stage in the review [22]. QD WLEDs based on core-shell QDs are first reviewed. White LEDs based on Cd-free QDs, as well as white LEDs based on phosphors and QDs together, fall under this category.

A WLED using transition-metal doped QDs, a relatively new type of QD-WLEDs, is the next step in our

investigation [9]. White LEDs based solely on core QDs will be the final topic of discussion. QD-WLEDs have been widely investigated for greater color quality and photometric efficiency since the earliest demonstrations of the usage of color converting QDs on LEDs a number of years ago, and their overall performance has been improved over the years.

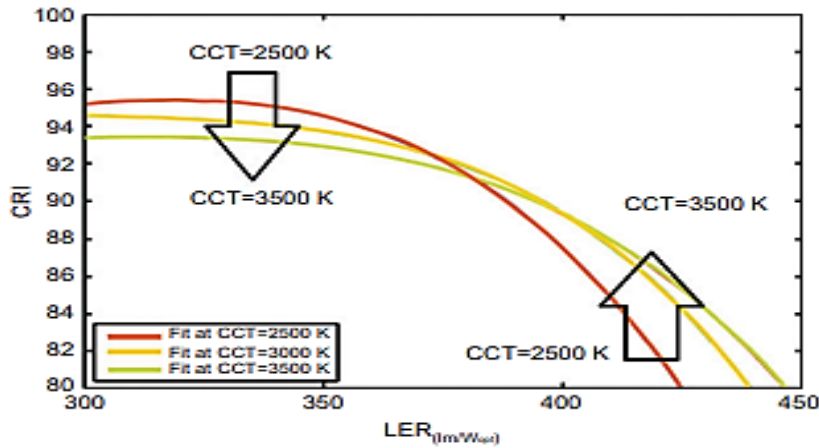


Fig. 3 – CRI vs. LER relationship at CCTs of 2500, 3000, and 4000 K

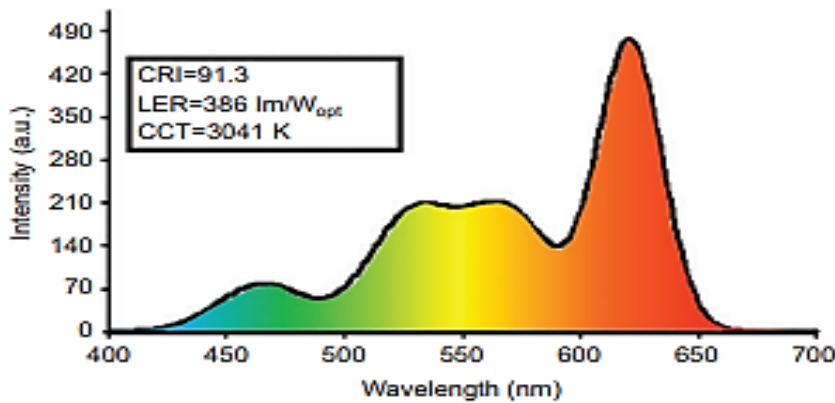


Fig. 4 – QD-WLED spectrum generated using the average values obtained by applying thresholds of CRI > 90, LER > 380 lm/W_{opt}, and CCT < 4000 K along with its photometric performance

Table 1 – Optimal spectral parameters of QD-WLEDs leading to the highest LERs satisfying CRI = 95 and R9 = 95 at 1500 K ≤ CCT ≤ 6500 K

CCT (K)	2700	3000	3500	4000	4500	5000	5700	6500
Blue WL	462.5	462.3	461.6	460.9	460.2	461.1	460.4	459.7
Green WL	520.9	521.6	522.4	522.9	523.3	523.7	523.9	523.9
Yellow WL	566.0	566.0	566.2	566.6	567.0	566.7	567.4	568.2
Red WL	623.7	623.0	622.1	621.5	621.0	620.7	620.4	620.1
Blue FWHM	30	30	30	30	30	30	30	30
Green FWHM	30	30	30	30	30	30	30	30
Yellow FWHM	30	30	30	30	30	30	30	30
Red FWHM	30	30	30	30	30	30	30	30
Blue amplitude (%)	7.82	10.67	15.13	19.00	22.37	24.77	28.22	31.31
Green amplitude (%)	15.72	17.65	20.24	22.20	23.63	25.00	25.99	26.67
Yellow amplitude (%)	27.10	26.57	25.18	23.64	22.17	20.82	19.40	18.12
Red amplitude (%)	49.36	45.11	39.46	35.16	31.83	29.42	26.40	23.90
CRI	95	95	95	95	95	95	95	95
R9	95	95	95	95	95	95	95	95
CQS	93	94	94	93	93	93	93	93
LER (IM/W _{opt})	370	371	367	360	352	347	338	327

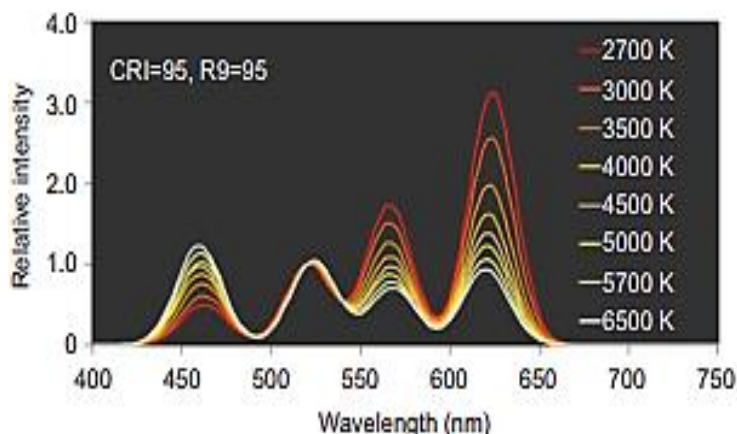


Fig. 5 – QD-WLEDs with the best spectra for the highest LERs CRI = 95 and R9 = 95 at $1500\text{ K} \leq \text{CCT} \leq 6500\text{ K}$

A blue LED with CdSe/ZnS QDs was used in one of the initial studies. According to Demir and his team, the CCT may be adjusted between 2692 K and 11.171 K utilizing combinations of cyan, green, orange, or red QDs on the blue LED chip. This material system was used again one year later, and researchers improved its performance by a factor of two. The QD-WLEDs have a CRI of 81, an LER of 323 lm/W opt, and a CCT of 3190 K, according to reports. Fig. 6 shows the white LED spectrum in order to achieve these results.

A blue LED chip was used to increase the QD-WLED performance by incorporating green, yellow, and red CdSe/ZnS QDs, each emitting at 528, 560 and 609 nm in toluene. With an LER of 357 lm/W opt, a CRI of 89.2 and a CCT of 2982 K, this particular device was able to meet all of its specifications. Fig. 7 shows the spectrum, color coordinates, and a picture of this QD-WLED. Nizamoglu et al. employed CdSe/ZnS QDs to make white LEDs that had a high S/P ratio and good CRI in another investigation. In that particular study, the designed QD-WLED exhibited an S/P ratio of 3.04 with a CRI of 71 at CCT = 45.000 K.

While CdSe/ZnS core/shell topologies were studied for QD-WLED production, alternative QD designs were also researched. With a dual-color emission, the QD-WLED integrated with ZnSe (CdSe) core, shell, and shell QDs is one of the most fascinating ones. However, the second shell of the QD was predicted to produce green emission. Using these QDs in conjunction with an InGaN/GaN blue LED, white light emission was

made possible (Fig. 8). The CRI = 75.1, LER = 278 lm/W opt, and CCT = 3929 K.

2. MATERIALS AND METHODS

2.1 Materials and Experimental Setup

Classical mechanics is no longer sufficient to describe the behavior of materials as they shrink in size; instead, the governing mechanisms rely on quantum physics concepts. The same basic principles apply to semiconductor nanocrystal QDs. The electrons and holes in a semiconductor QD are typically restricted to a region of 2-10 nm in three dimensions. In semiconductors, electrons and holes are typically separated by this distance. Consequently, crystalline semiconductor electrons and holes begin to see the surrounding free space or any other material with a greater band gap as a barrier. This results in a finite quantum well problem, in which discrete energy levels control the material properties of the system.

It is difficult to inject a charge into the QDs because of the massive barriers created by organic ligands surrounding them, which serve primarily to passivate the QD surface. It is therefore difficult to inject carriers into QDs, resulting in lower overall device efficiency. There have been tremendous advancements in the previous decade despite this challenge, for long-term operation; there are concerns about charge accumulation and photo charging effects.

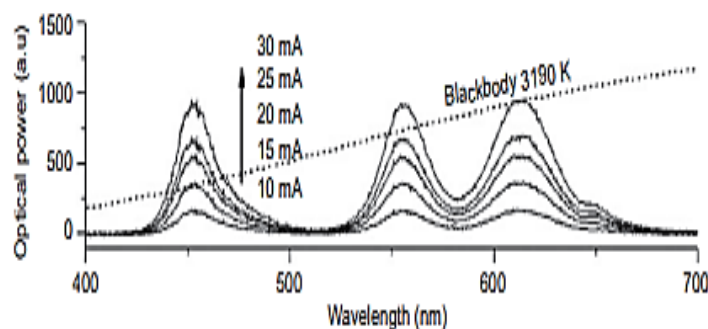


Fig. 6 – White LEDs constructed using CdSe/ZnS QDs on blue InGaN/GaN LEDs have been measured. The QD-WLED has the following performance characteristics: CRI = 81, LER = 323 lm/W opt, and CCT = 3190 K

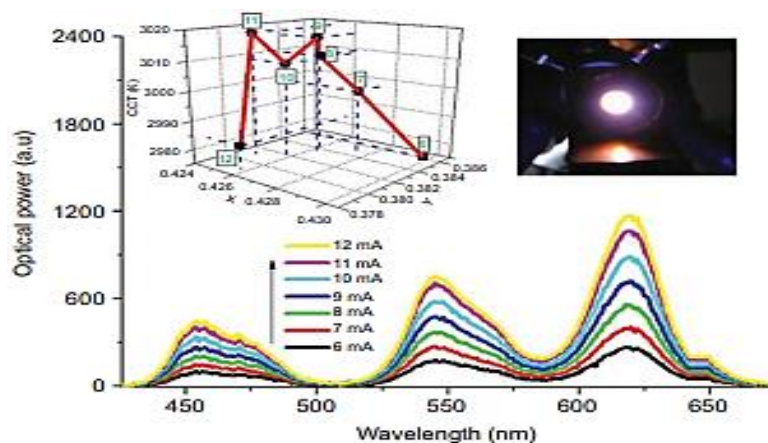


Fig. 7 – Figure-of-merits of WLED with CdSe/ZnS QD integration measured spectra, chromaticity coordinates, and photograph of CRI = 89.2, LER = 357 lm/W opt, and CCT = 2982 K

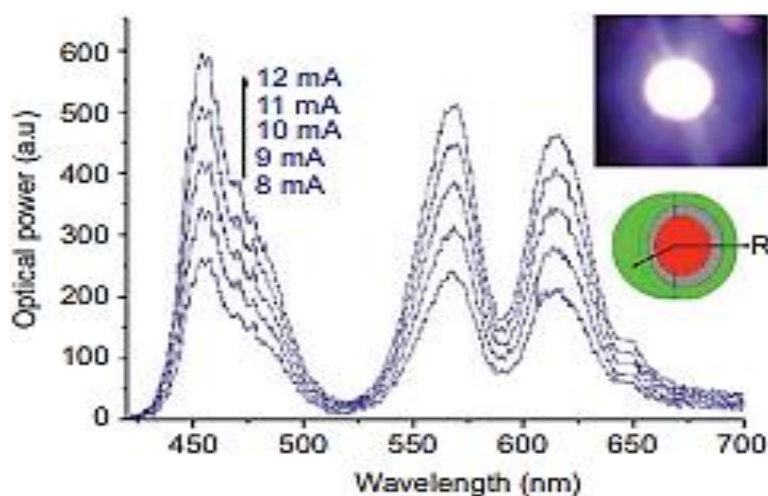


Fig. 8 – Spectra and photograph of the (CdSe)ZnS/CdSe (core) shell/shell QD-integrated WLED

2.2 Chemicals Required

Chemicals used for the experiment were graphite powder (60 meshes), sulfuric acid (H_2SO_4), potassium permanganate (KMnO_4), hydrogen peroxide (of 30 % purity), sodium nitrate (NaNO_3), titanium di-oxide (TiO_2) and ethanol ($\text{C}_2\text{H}_5\text{OH}$). The required dyes and chemicals were purchased from K.M.P. Dyes and Chemicals, Tirupur. All chemicals are of analytical reagent (AR) grade.

2.3 Photochemical Reactivity

The filtered water samples for photochemical reactivity measurements were incubated under UV irradiation ($3.64\text{-}6.89\text{ Wm}^{-2}$ for UV-A and $0.06\text{-}0.1\text{ Wm}^{-2}$ for UV-B) for 48 h [24]. More details of the experiment are available elsewhere. Briefly, 10 ml aliquots of the filtered water sample were filled in 20 ml quartz vials and the remaining 10 ml (headspace) was filled with a synthetic air mixture. For each sample, two vials were kept as control and acidified immediately with 0.1 ml of concentrated H_3PO_4 , and two additional vials were incubated at $20\pm 1\text{ }^\circ\text{C}$ under UV irradiation for 48 h. After irradiation, samples were acidified with 0.1 ml of concentrated H_3PO_4 to convert the dissolved inorganic

carbon (DIC) in the vials to CO_2 , shaken for a minute, and then left for a day to attain equilibrium. After equilibrium, 5 ml of the air samples were injected into EGM-4 infrared gas analyzer (PP systems, Amesbury, MA, USA) to measure CO_2 in headspace, and the DIC was calculated by accounting for the partitioning of CO_2 between the headspace and liquid phase of the sample. The DIC produced during incubation was calculated as the difference between the DIC observed after incubation and DIC from the control vials.

$$E_w = T_{UV} \sum_{\lambda=300}^{\lambda=550} I_{0\lambda} (1 - 10^{-\alpha})_{\lambda}, \quad (1)$$

$$(1 - 10^{-\alpha})_{\lambda} = \sum_I^{10} (1 - 10^{-\alpha L}) / 10. \quad (2)$$

E_w (J m^{-2}) was calculated based on the lamp energy in Wm^{-2} ($I_0\lambda$), incubation time in seconds (T_{UV}) and the average absorption of irradiation in the quartz vials at a specific wavelength ($[1 - 10^{-\alpha}]\lambda$). In order to account for the impact of self-shading within the quartz vials, we horizontally divided the quartz vial into ten different sections and calculated the mean irradiation path length of different section of the vial (L , cm) at each wavelength (Eq. (1) and Eq. (2)). It should be noted

that the mean vertical path length in our horizontally placed sample vials was short (0.81 cm) and does not represent the total depth of the water column that would be irradiated in nature. Thus, our photoreactivity variable $PD-E_w$ informs quantitatively about the photo-reactivity per unit of total light absorbed in 0.81 cm depth intervals of the water column in nature.

2.4 Photocatalytic Experiment

A hexagonal UV multi-lamp photoreactor (Heber scientific) with 100 ml capacity made of borosilicate glass having dimensions 35 cm \times 2 cm (height \times diameter) was used [24]. The experiment was carried out at ambient temperatures. The photocatalytic activity of the photocatalyst was evaluated by decolorizing orange ME2RL. 10 mg of photocatalyst was dispersed into 50 ml of aqueous solution containing 100 mg/l orange ME2RL dye. The mixture was stirred incessantly using an aerator under UV light. The concentration of orange ME2RL was measured by using a UV-Vis spectrophotometer at an interval of 5 min.

3. RESULTS AND DISCUSSION

While QD-WLED performance investigations continue, research efforts have begun to focus on synthesizing QDs in environmentally benign and cost-effective manners. Because QDs are synthesized using the phosphine group, they have a higher cost and are more damaging to the environment than other types of semiconductors [25]. CdSe/CdS/ZnS core/shell/shell QDs in paraffin liquid were synthesized and employed in WLED lights to overcome this issue. Quantum efficiency (QE) of the green QDs was 55 %, whereas the yellow and red QDs had peak emission wavelengths of 563 nm and 615 nm, respectively, with QEs of 66 % and 40 %. A CRI of 88 and a CCT of 3865 K were achieved with a luminous efficiency (LE) of 32 lm/W_{elect} in the manufactured device [26].

The Cd concentration of common QD materials is another major issue. New procedures are being developed for the production of Cd-free QDs in order to generate ecologically acceptable QDs. For example, the emission peaks of the CuInS/ZnS core shell QD can be altered by adjusting its indium content. Color rendering index (CRI) of 72 and a light output of 79.3 lm/W_{elect} were achieved by using CuInS/ZnS QDs with Cu/In ratios of 1/4. Fig. 9 depicts the LED resulting spectrum. QDs that generate yellow and orange light were utilized in a different Song et al. study for the creation of white light. As a result, the CRI was improved to 80-82 and the LE was improved to 52 lm/W_{elect} [27].

Researchers have researched the InP/ZnS core/shell QDs extensively as another key Cd-free QD. These materials' synthesis and device applications have seen major advancements in the last several years. A WLED with a CRI of 89.3 at a CCT of 2982 K and an LER of 254 lm/W_{opt} was demonstrated in the work of Mutlugun et al. Fig. 10 shows the QD-spectrum WLED and a picture of the device [28].

InP/ZnS, InP/ZnSe, and InP/ZnSSe QDs are plagued by a lattice mismatch between the core and shell materials, which inhibits QE. Core/shell/shell QDs, as proposed by Kim et al., were a solution. With the 85 % QE, these QDs displayed WLEDs produced from yttrium aluminum garnet phosphor (YAG). At a CCT of 7864 K, this QD-WLED has a CRI of 80.56 and an LE of 54.71 lm/W_{elect}. One thing to keep in mind, however, is that the use of QDs in phosphors is not unique. Sr₂SiO₄:Eu green phosphor was combined with red QDs of CdSe/CdS, ZnS, and Sr on an InGaN/GaN blue LED by Woo and colleagues. At 617 nm, QDs had a FWHM of 32 nm and a quantum efficiency of more than 55 percent. At a CCT of 8684 K, this device had a CRI of 88.4 and an elect luminous efficiency of 71.2 lm/W. Fig. 11 shows the spectrum and an image of this particular gadget [29].

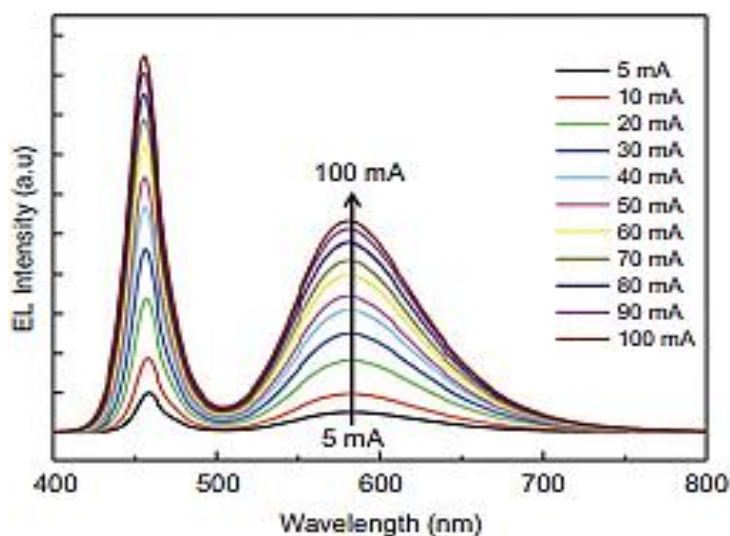


Fig. 9 – Spectra of the QD-WLED based on CuInS/ZnS core/shell QDs exhibiting a CRI of 72 and an LE of 79.3 lm/W_{elect}

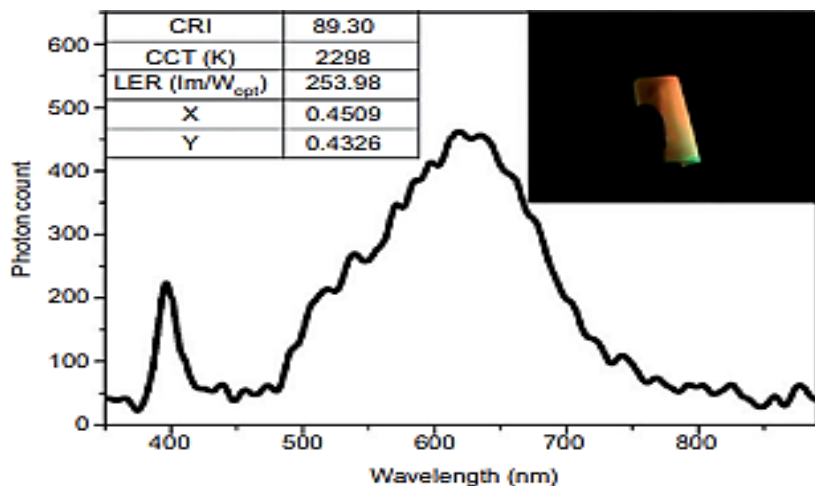


Fig. 10 – Spectra of the QD-WLED based on InP/ZnS QDs, its colorimetric and photometric performance (left), and a photograph of the QD-WLED (right)

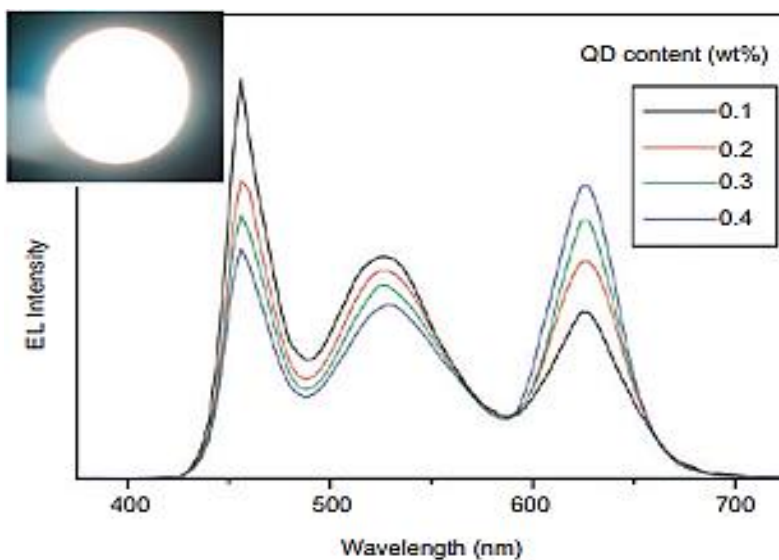


Fig. 11 – Sr₂SiO₄:Eu phosphors and red QDs of CdSe/CdS/CdZnS/ZnS at 30 mA with different QD concentrations in a QD-WLED. A photograph of the device is shown in the inset

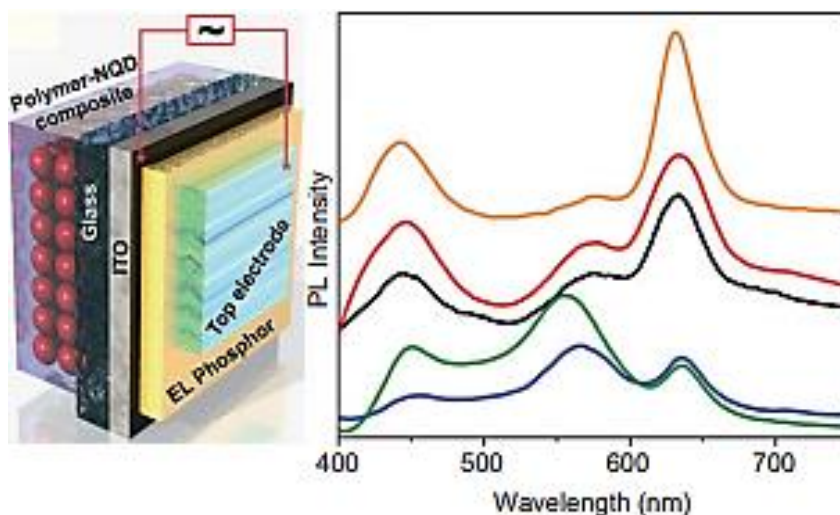


Fig. 12 – Phosphor-integrated color-changing QDs (left) and their electroluminescence spectrum of LEDs with varying concentrations of green and red QDs (right)

In addition to being used as down-converters on electroluminescent phosphors, QDs were also used as color converters on an epitaxially produced blue LED. When Kundu et al. studied the red emissive nanophosphors at 625 nm using the so-called huge CdSe/CdS QDs with 16 monolayers of shells, they found that they were emitting green light from InP/ZnSe QDs on an electroluminescent blue phosphor powder made of Cu/Cl-doped ZnS. The CCTs of the white LED were tuned between 3200 and 5800 K by using these materials. Fig. 12 shows the concept of the device, as well as the electroluminescence spectra [8].

4. CONCLUSIONS

In conclusion, quantum-dot-integrated white LEDs (QD-WLEDs) based on color conversion have been the subject of recent research. A foundation in color science and photometry was laid out first in order to evaluate white light sources' performance. After that, we examined the spectrum design of QD-WLEDs and the parameters required for high performance. The next step

was to demonstrate QD-WLEDs in an experimental setting for general illumination and displays. According to this research, QD-WLEDs have a lot of potential for both indoor and outdoor lighting applications. A color rendering index (CRI) close to 90, good overlap with the human eye sensitivity curve, and an optical radiation efficacy greater than 350 lm/W opt are all achievable with these devices at the same time, unlike other conventional sources such as fluorescent and incandescent bulbs. High photometric performance and color quality have been achieved in combination with efficient QD synthesis, leading to QD-WLEDs with efficiency close to 80 lm/W elect. However, there is still room for improvement up to 315 lm/W elect, which has been theoretically shown to be possible without compromising on color quality or photometric quality. In addition, their usage in screens makes it possible to reproduce colors extremely well. Using QD-WLEDs as display backlights allows for a wider color gamut than that needed by NTSC standards due to the narrow emission bands that QDs can provide.

REFERENCES

1. D.I. Halliday, R. Peon, G. Doluweera, A. Platonova, G.I. Halliday, *SPIE* (2006).
2. N.H. Moadab, T. Olsson, G. Fischl, M. Aries, *Energy Build.* **244**, 111009 (2021).
3. A. Bergh, G. Craford, A. Duggal, R. Haitz, *Phys. Today* **54** No 12, 42 (2001).
4. L. Liu, G.A. Keoleian, K. Saitou, *Environ. Res. Lett.* **12**, 114034 (2017).
5. C. Weisbuch, *C.R. Phys.* **19** No 3, 89 (2018).
6. S. Ye, X. Feiyum, Y.X. Pan, Y.Y. Ma, Q.Y. Zhang, *Mater. Sci. Eng. R* **71** No 1, 1 (2010).
7. A. David, L.A. Whitehead, *C.R. Phys.* **19** No 3, 169 (2018).
8. T. Erdem, H. Demir, *Nat. Photon.* **5**, 126 (2011).
9. E. Jang, S. Jun, H. Jang, J. Lim, B. Kim, Y. Kim, *Adv. Mater.* **22** No 28, 3076 (2010).
10. T. Erdem, S. Nizamoglu, H.V. Demir, *Opt. Exp.* **20**, 3275 (2012).
11. S. Bayda, M. Adeel, T. Tuccinardi, M. Cordani, F. Rizzolio, *Molecules* **25** No 1, 112 (2020).
12. R.E. Bailey, S. Nie, *J. Am. Chem. Soc.* **125** No 23, 7100 (2003).
13. B.V. Lopushanska, Y.M. Azhniuk, I.P. Studenyak, V.V. Lopushansky, A.V. Gomonnai, D.R.T. Zahn, *J. Nano-Electron. Phys.* **14** No 4, 04010 (2022).
14. C.T. Jackson, S. Jeong, G.F. Dorlhiac, M.P. Landry, *iScience* **24** No 3, 102156 (2021).
15. T. Kruisselbrink, R. Dangol, A. Rosemann, *Buil. Environ.* **138**, 42 (2018).
16. J. Enoch, L. Jones, D.J. Taylor, C. Bronze, J.F. Kirwan, P.R. Jones, D.P. Crabb, *Eye* **34** No 1, 138 (2020).
17. P. Moraitis, R.E.I. Schropp, W.G.J.H.M. Van Sark, *Opt. Mater.* **84**, 636 (2018).
18. G. He, L. Zheng, *Opt. Lett.* **35** No 17, 2955 (2010).
19. T. Erdem, S. Nizamoglu, X.W. Sun, H.V. Demir, *Opt. Exp.* **18**, 340 (2010).
20. P. Zhong, G. He, M. Zhang, *Opt. Exp.* **20** No 8, 9122 (2012).
21. T. Wu, Y. Lu, Z. Guo, L. Zheng, H. Zhu, Y. Xiao, T. Shih, Y. Lin, Z. Chen, *Opt. Exp.* **25** No 5, 4887 (2017).
22. T. Erdem, H.V. Demir, *Nanophotonics* **2** No 1, 57 (2013).
23. B.P. Selvam, J.F. Lapierre, A.R.A. Soares, D.T. Bastviken, J. Karlsson, M. Berggren, *Aquat. Sci.* **81** No 4, 57 (2019).
24. P.C.S. Bezerra, R.P. Cavalcante, A. Garcia, H. Wender, M.A.U. Martinez, G.A. Casagrande, J. Gimenez, M. Pilar, S.D. Oliveira, A. Machulek, *J. Braz. Chem. Soc.* **28** No 9, 1 (2017).
25. D. Bera, L. Qian, T.K. Tseng, P.H. Holloway, *Materials* **3** No 4, 2260 (2010).
26. X. Wang, W. Li, K. Sun, *J. Mater. Chem. A* **21** No 24, 8558 (2011).
27. H.M. Gil, T.W. Price, K. Chelani, J.S.G. Bouillard, S.D.J. Calaminus, G.J. Stasiuk, *iScience* **24** No 3, 102189 (2021).
28. K. Kim, S. Jeong, J.Y. Woo, C.S. Han, *Nanotechnology* **23** No 6, 065602 (2012).
29. C. Ippen, T. Greco, A. Wedel, *J. Inf. Disp.* **13** No 2, 91 (2012).

Дослідження фотореактивності неорганічних нанокристалів зі значними органічними кольорами

K. Umamakeshvari¹, S.C. Vella Durai², M. Nagarajan³

¹ Christopher Arts and Science College (Women), Nanguneri, Tirunelveli, 627108 Tamilnadu, India

² Manonmaniam Sundaranar University College, Govindaperi, Cherenmahadevi, Tirunelveli, 627414 Tamilnadu, India

³ Government Arts and Science College, Kanyakumari, 629401 Tamilnadu, India

Серед фотонних оптоелектронних матеріалів особливо можна виділити колоїдні нанокристали напівпровідникових квантових точок (QDs). Завдяки своїй високій ефективності та вузькій смузі випромінювання, спектральній чистоті та можливості точного налаштування вони широко використовуються у штучному освітленні та дисплеях. В результаті використання QDs в кольороперетворювальних світлодіодах у поєднанні з люмінофорами вдається одночасно досягти вдалої кольоропередачі об'єктів, що освітлюються. Спектральне перекриття пристрою з чутливістю людського ока є видатним, на відміну від інших традиційних джерел, таких як лампи розжарювання та люмінесцентні лампи, а також світлодіодів на основі люмінофора, які не можуть забезпечити всі вищезазначені характеристики одночасно. Кольорознавство QDs для освітлення та дисплеїв підсумовується в цій статті разом із останніми досягненнями в світлодіодах на основі інтегрованих QDs та дослідженнях дисплеїв. Кольорознавство, фотометрія та радіометрія представлені в першому розділі. Спектральні конструкції білих світлодіодів на основі інтегрованих QDs призвели до ефективного як внутрішнього, так і зовнішнього освітлення. Кольороперетворювальні світлодіоди на основі QDs та дисплеї обговорюються як докази концепції в наступному розділі. У заключенні ми представляємо огляд дослідницьких можливостей і труднощів, а також прогноз на майбутнє.

Ключові слова: Кольорознавство, Дисплеї, Світлодіоди, Нанокристали, Фотометрія, Квантові точки.